2011-09-01

Veritas Observations Of The Tev Binary Ls I+61 Degrees 303 During 2008-2010

P. T. Reynolds
Cork Institute of Technology

Et. al.

Recommended Citation

Acciari, V. A. et al. (2011) 'VERITAS OBSERVATIONS OF THE TeV BINARY LS I +61° 303 DURING 2008-2010', The Astrophysical Journal, 738(1), p. 3. doi: 10.1088/0004-637X/738/1/3.

The Astrophysical Journal, 738:3 (8pp), 2011 September 1 doi:10.1088/0004-637X/738/1/3

VERITAS OBSERVATIONS OF THE TeV BINARY LS I +61° 303 DURING 2008–2010

V. A. Acciari[1], E. Aliu[2], T. Arlen[3], T. Aune[4], M. Beilicke[5], W. Benbow[1], S. M. Bradbury[6], J. H. Buckley[5], V. Bugaev[5], K. Byrum[7], A. Cannon[8], A. Cesarini[9], L. Ciupik[10], E. Collins-Hughes[8], M. P. Connolly[9], W. Cui[11], R. Dickherber[5], C. Duke[12], M. Errando[2], A. Falcone[13], J. P. Finley[11], G. Finnegan[14], L. Fortson[15], A. Furniss[4], N. Galante[1], D. Gall[11], G. H. Gillanders[9], S. Godambe[14], S. Griffin[16], J. Grube[10], R. Guenette[16], G. Gyuk[10], D. Hanna[16], J. Holder[17,28], G. Hughes[18], C. M. Hui[14], T. B. Humensky[19], P. Kaaret[20], N. Karlsson[15], M. Kertzman[21], D. Kieda[14], H. Krawczynski[5], F. Krennrich[22], M. J. Lang[9], S. LeBohec[14], G. Maier[18], P. Majumdar[3], S. McArthur[5], A. McCann[16], P. Moriarty[23], R. Mukherjee[2], R. A. Ong[3], M. Orr[22], A. N. Otte[4], N. Park[19], J. S. Perkins[1], M. Pohl[18,24], H. Prokoph[18], J. Quinn[8], K. Ragan[16], L. C. Reyes[19], P. T. Reynolds[25], E. Roache[1], H. J. Rose[6], J. Ruppel[24], D. B. Saxon[17], M. Schroedter[22], G. H. Sembroski[11], G. D. Senturk[26], A. W. Smith[7,27,28], D. Staszak[16], G. Tešić[16], M. Theiling[1], S. Thibadeau[5], K. Tsurusaki[20], A. Varlotta[11], V. V. Vassiliev[3], S. Vincent[14], M. Vivier[17], S. P. Wakely[19], J. E. Ward[8], T. C. Weekes[1], A. Weinstein[3], T. Weisgarber[19], D. A. Williams[4], and B. Zitzer[11]

[1] Fred Lawrence Whipple Observatory, Harvard-Smithsonian Center for Astrophysics, Amado, AZ 85645, USA
[2] Department of Physics and Astronomy, Barnard College, Columbia University, NY 10027, USA
[3] Department of Physics and Astronomy, University of California, Los Angeles, CA 90095, USA
[4] Santa Cruz Institute for Particle Physics and Department of Physics, University of California, Santa Cruz, CA 95064, USA
[5] Department of Physics, Washington University, St. Louis, MO 63130, USA
[6] School of Physics and Astronomy, University of Leeds, Leeds, LS2 9JT, UK
[7] Argonne National Laboratory, 9700 S. Cass Avenue, Argonne, IL 60439, USA; awsmith@hep.anl.gov
[8] School of Physics, University College Dublin, Belfield, Dublin 4, Ireland
[9] School of Physics, National University of Ireland Galway, University Road, Galway, Ireland
[10] Astronomy Department, Adler Planetarium and Astronomy Museum, Chicago, IL 60605, USA
[11] Department of Physics, Purdue University, West Lafayette, IN 47907, USA
[12] Department of Physics, Grinnell College, Grinnell, IA 50112-1690, USA
[13] Department of Astronomy and Astrophysics, 525 Davey Lab, Pennsylvania State University, University Park, PA 16802, USA
[14] Department of Physics and Astronomy, University of Utah, Salt Lake City, UT 84112, USA
[15] School of Physics and Astronomy, University of Minnesota, Minneapolis, MN 55455, USA
[16] Physics Department, McGill University, Montreal, QC H3A 2T8, Canada
[17] Department of Physics and Astronomy and the Bartol Research Institute, University of Delaware, Newark, DE 19716, USA; jholder@physics.udel.edu
[18] DESY, Platanenallee 6, 15738 Zeuthen, Germany
[19] Enrico Fermi Institute, University of Chicago, Chicago, IL 60637, USA
[20] Department of Physics and Astronomy, University of Iowa, Van Allen Hall, Iowa City, IA 52242, USA
[21] Department of Physics and Astronomy, DePauw University, Greencastle, IN 46135-0037, USA
[22] Department of Physics and Astronomy, Iowa State University, Ames, IA 50011, USA
[23] Department of Life and Physical Sciences, Galway-Mayo Institute of Technology, Dublin Road, Galway, Ireland
[24] Institut für Physik und Astronomie, Universität Potsdam, 14476 Potsdam-Golm, Germany
[25] Department of Applied Physics and Instrumentation, Cork Institute of Technology, Bishopstown, Cork, Ireland
[26] Columbia Astrophysics Laboratory, Columbia University, New York, NY 10027, USA
[27] Department of Physics and Astronomy, Northwestern University, Evanston, IL 60208, USA
Received 2011 February 22; accepted 2011 May 1; published 2011 August 9

ABSTRACT

We present the results of observations of the TeV binary LS I +61° 303 with the VERITAS telescope array between 2008 and 2010, at energies above 300 GeV. In the past, both ground-based gamma-ray telescopes VERITAS and MAGIC have reported detections of TeV emission near the apastron phases of the binary orbit. The observations presented here show no strong evidence for TeV emission during these orbital phases; however, during observations taken in late 2010, significant emission was detected from the source close to the phase of superior conjunction (much closer to periastron passage) at a 5.6 standard deviation (5.6σ) post-trials significance. In total, between 2008 October and 2010 December a total exposure of 64.5 hr was accumulated with VERITAS on LS I +61° 303, resulting in an excess at the 3.3σ significance level for constant emission over the entire integrated data set. The flux upper limits derived for emission during the previously reliably active TeV phases (i.e., close to apastron) are less than 5% of the Crab Nebula flux in the same energy range. This result stands in apparent contrast to previous observations by both MAGIC and VERITAS which detected the source during these phases at 10% of the Crab Nebula flux. During the two year span of observations, a large amount of X-ray data were also accrued on LS I +61° 303 by the *Swift* X-ray Telescope and the *Rossi X-ray Timing Explorer* Proportional Counter Array. We find no evidence for a correlation between emission in the X-ray and TeV regimes during 20 directly overlapping observations. We also comment on data obtained contemporaneously by the *Fermi* Large Area Telescope.

Key words: binaries: general – gamma rays: general – X-rays: binaries

Online-only material: color figures

1. INTRODUCTION

The high-mass X-ray binary LS I +61° 303 is one of only three such systems firmly identified as a source of TeV gamma rays. Despite many years of observations across the electromagnetic spectrum, the system remains, in some respects, poorly characterized. Known to be the pairing of a massive B0 Ve star and a compact object of unknown nature (Hutchings & Crampton 1981; Casares et al. 2005), LS I +61° 303 has been known historically for its energetic outbursts at radio, X-ray, GeV, and TeV wavelengths (Gregory et al. 2002; Greiner & Rau 2001; Harrison et al. 2000; Abdo et al. 2009; Albert et al. 2008; Acciari et al. 2008), all of these showing correlation with the 26.5 day orbital cycle of the compact object in its path around the Be star. According to the most recent radial velocity measurements, the orbit is elliptical ($e = 0.537 \pm 0.034$), with periastron passage determined to occur around phase $\phi = 0.275$, apastron passage at $\phi = 0.775$, superior conjunction at $\phi = 0.081$, and inferior conjunction at $\phi = 0.313$ (Aragona et al. 2009). The non-thermal behavior of the source is well studied, yet poorly understood. The radio emission presents a well-defined periodicity with strong flares occurring periodically near apastron passage, along with an additional modulation on a 4.6 year timescale (Gregory 2002). The detection of extended structures in radio observations originally identified LS I +61° 303 as a potential microquasar, with high energy (HE) emission produced in jets driven by accretion onto the compact object, presumably a black hole (Massi et al. 2001). High-resolution Very Long Baseline Array (VLBA) observations indicate that the radio structures are not persistent, however, and can be more easily explained by the interaction between a pulsar wind and the wind of the stellar companion (Dhawan et al. 2006; Albert et al. 2008), although alternative interpretations are still possible (Romero et al. 2007; Massi & Zimmerman 2010). The full range of arguments in favor of LS I +61° 303 as a non-accreting pulsar system has been summarized by Torres et al. (2011).

The X-ray behavior is well studied (see Smith et al. 2009 for a review), most comprehensively in Torres et al. (2010), in which the authors present an analysis of *Rossi X-ray Timing Explorer* Proportional Counter Array (*RXTE*–PCA) observations taken over four years, covering 35 full orbital cycles. They show that, while the X-ray emission from the source is indeed periodic, there is variability of the orbital profiles on multiple timescales, from individual orbits up to years. Additionally, intense X-ray flares have been observed (Smith et al. 2009; Torres et al. 2010), during which the flux increases by up to a factor of five and variability on the timescale of a few seconds is observed. It is noted, however, that due to the relatively large *RXTE*–PCA field of view (~1° FWHM), the possibility that these flares are due to an unrelated source in the same field cannot be ruled out.

HE (30 MeV–30 GeV) gamma-ray emission, spatially coincident with LS I +61° 303, although with large positional errors, was first detected by COS-B (Hermsen et al. 1977) and, subsequently, by EGRET (Tavani et al. 1998). The detection of a variable very high energy (VHE; 30 GeV–30 TeV) gamma-ray source at the location of LS I +61° 303 with MAGIC (Albert et al. 2006), later confirmed by VERITAS (Acciari et al. 2008), completed the identification of this source as a gamma-ray binary. The TeV emission reported by both experiments for observations made prior to 2008 is spread over approximately one quarter of the orbit, with a peak around apastron (orbital phase $\phi = 0.775$). *Fermi* Large Area Telescope (LAT) observations provide the definitive HE detection and have revealed a number of interesting features (Abdo et al. 2009). The HE emission reported in the detection paper (based on observations from 2008 August until 2009 March) is modulated at the orbital period (peaking slightly after periastron ($\phi = 0.225$)), although recent results from the LAT show different behavior (see the summary and discussion). The overall *Fermi* spectrum shows a sharp exponential cutoff at 6 GeV.

The existence of orbital modulation in the gamma-ray flux is often explained by the varying efficiency of the inverse Compton process around the orbit, although we note that many alternative explanations exist (see, e.g., Sierpowska-Bartosik & Torres 2009 for a review). In this scenario, inverse Compton gamma-ray production along our line of sight is most efficient at superior conjunction ($\phi = 0.081$), where stellar photons interact head-on with energetic leptons produced either directly in the pulsar wind or in the pulsar wind/stellar wind shock interaction region. The density of stellar photons may also play a role in the efficiency of gamma-ray production, with the highest density occurring at periastron. The TeV flux is further modulated by photon–photon absorption around the orbit, which peaks near superior conjunction and may dominate over the modulation effects due to production efficiency at energies above ~30 GeV. Orbital modulation of the GeV and TeV fluxes, with large differences between the light curves observed in each energy band, is therefore not unexpected. Other effects, for example Doppler boosting of the emission (Dubus et al. 2010), clumps in the wind of the Be star (Araudo 2009), tidal disruption of the accretion disk (Romero et al. 2007), or cascading of HE photons to lower energies, may also play a role and provide a better fit of the models to the observations. However, it should be noted that the orbital inclination of the system is poorly constrained, and this complicates the modeling of emission from this system.

Substantial effort has been invested in constructing multi-wavelength data sets on LS I +61° 303. Preliminary studies including TeV data (Acciari et al. 2009; Albert et al. 2008) combined long-term (multi-orbit) observations at both X-ray and TeV wavelengths. Acciari et al. (2009) did not detect any correlation between emission at X-ray and TeV wavelengths with observations taken by VERITAS, *Swift*–X-ray Telescope (XRT), and *RXTE*–PCA. However, the multiwavelength observations used were not strictly overlapping, which is problematic given the observed fast (several seconds) variability in the X-ray regime detailed in Smith et al. (2009). Further X-ray/TeV observations reported in Anderhub et al. (2009) detect a correlation between X-ray and TeV emission during a TeV outburst over a single orbital cycle. While the authors show a correlation (with a 0.5% probability of being produced from independent data sets), the longer-scale correlation behavior of the source outside of the observed flare is not well studied.

In this paper, we summarize the results of VERITAS observations of LS I +61° 303 between 2008 and 2010, including a comparison with strictly contemporaneous X-ray observations. These are the first reported TeV observations since the launch of *Fermi* in 2008 June, and so they provide an opportunity to examine the broadband HE (100 MeV–10 TeV) emission from the source using contemporaneous observations.

2. VERITAS OBSERVATIONS

The VERITAS array of imaging atmospheric Cerenkov telescopes (IACTs), located in southern Arizona (1250 m a.s.l., 31°40′N, 110°57′W), is composed of four, 12 m diameter, 12 m

[28] Author to whom any correspondence should be addressed.

Table 1
VERITAS Observations of LS I +61° 303 in the 2008–2009 Observing Season

MJD (UTC)	Phase (ϕ)	Livetime (minutes)	Significance σ	Flux/99% U.L.> 300 GeV (10^{-12} γ cm^{-2} s^{-1})
54760.3	0.03	113.6	2.2	<10.1
54761.4	0.07	89.6	1.7	<9.9
54762.3	0.1	90.2	0.6	<6.8
54763.4	0.15	18.1	−0.4	<10.3
54764.2	0.18	111.5	0.5	<4.4
54765.2	0.22	126.9	−1.4	<2.6
54766.2	0.26	90.4	0.2	<5.9
54767.3	0.31	36.1	0.2	<6.9
54768.3	0.35	90.7	0.4	<6.0
54769.3	0.37	109.7	−0.3	<2.9
54770.3	0.41	54.7	−0.9	<4.4
54771.3	0.44	72.8	1.0	<6.5
54772.3	0.48	72.9	1.7	<10.2
54774.3	0.56	90.7	2.7	<9.2
54775.3	0.59	54.1	−0.7	<4.4
54776.3	0.63	162.5	1.5	<4.4
54777.4	0.67	72.5	0.5	<7.2
54778.4	0.71	54.4	−0.8	<5.8
54779.4	0.75	36.5	−0.3	<7.8
54856.1	0.64	102.9	0.4	<6.1
54857.1	0.68	90.5	−1.8	<2.7
54861.1	0.83	95.2	1.1	<7.4
54862.1	0.87	104.0	0.9	<6.8
54863.1	0.91	76.1	1.4	<8.8

focal length telescopes, each with a Davies–Cotton tessellated mirror structure of 345 mirror facets (total mirror area of 110 m^2; Ong et al. 2009). Each telescope focuses Cerenkov light from particle showers onto a 499 pixel photomultiplier tube (PMT) camera. The pixels have an angular spacing of 0°.15, resulting in a camera field of view of 3°.5. During the summer months of 2009, one of the telescopes in the array was relocated, creating a more symmetric array layout and increasing the sensitivity of the observatory by 30% (Perkins et al. 2009). In its current configuration, VERITAS is able to detect a source with a flux of 1% of the steady Crab Nebula flux in under 30 hr. VERITAS has the capability to detect and measure gamma rays in the 100 GeV–30 TeV energy regime with an energy resolution of 15%–20% and an angular resolution of 0°.1 (68% containment) on an event-by-event basis.

The VHE observations presented here were made with VERITAS between 2008 October and 2010 December, sampling eight separate orbital cycles of the binary system. The data comprise 64.5 livetime hours of observations taken with both the original (33.3 hr) and current (31.2 hr) array configurations. Data were taken using the complete four-telescope array; Cerenkov images which trigger two or more telescopes initiate a readout of the 500 MSpS Flash-ADC data acquisition on each PMT. The observations were made in "wobble" mode in which the source is offset from the center of the field of view of the cameras to maximize efficiency in obtaining both source and background measurements (Fomin et al. 1994). After eliminating data taken under variable or poor sky conditions and applying image cleaning methods to reject images without sufficient signal for reconstruction, gamma-ray selection cuts were applied to the data. These selection cuts are based on the image morphology (*Mean Scaled Width* and *Length*), and the angular distance between the reconstructed position of the source in the camera plane and the a priori known source location. Cuts were optimized on simulated data for both the old and new array

Table 2
Same as Table 1, but for the 2009–2010 Observing Season

MJD (UTC)	Phase (ϕ)	Livetime (minutes)	Significance σ	Flux/99% U.L.> 300 GeV (10^{-12} γ cm^{-2} s^{-1})
55119.3	0.58	128.5	1.6	<7.3
55120.3	0.62	107.1	−0.4	<5.5
55121.3	0.65	161.6	−2.5	<1.6
55122.3	0.69	107.9	0.9	<6.0
55123.3	0.73	18.2	−0.7	<9.4
55124.3	0.77	99.2	1.9	<7.9
55146.2	0.59	146.3	3.4	5.8 ± 1.9
55151.2	0.78	123.2	2.1	<10.0
55175.2	0.69	54.7	−0.7	<6.5
55176.2	0.73	54.6	−0.3	<7.3
55177.2	0.76	18.2	−0.8	<10.3

Table 3
Same as Table 1, but for the 2010–2011 Observing Season

MJD (UTC)	Phase (ϕ)	Livetime (minutes)	Significance σ	Flux/99% U.L.> 300 GeV (10^{-12} γ cm^{-2} s^{-1})
55455.4	0.26	55.4	1.7	<10.08
55457.4	0.33	18.0	1.4	<18.00
55476.4	0.05	91.7	1.3	<11.4
55477.3	0.09	162.6	5.7	9.23 ± 1.9
55480.3	0.2	54.2	2.3	<19.7
55481.3	0.24	107.9	2.0	<9.3
55482.3	0.28	108.3	−0.3	<4.2
55483.3	0.32	128.1	−0.04	<5.84
55505.3	0.14	36.5	2.7	<23.7
55506.2	0.18	73.3	0.9	<11.09

configurations; the analysis presented here was performed with cuts optimized for the detection of a moderately weak (5% Crab Nebula flux) source. The data on LS I+61°303 were taken over a relatively small range of elevation angles (55°–60°) under dark skies (little or no moonlight) resulting in an energy threshold for these observations of 300 GeV.

In the entire integrated data set of 64.5 hr, 176 excess events above background were detected, corresponding to a 3.3σ statistical excess for steady emission, which does not constitute a significant detection. In Tables 1–3 and Figures 1–3 the results of the three years' observations are shown. For observations (both nightly, and binned by orbital phase) which did not exhibit a pre-trials excess above 3σ, 99% confidence level flux upper limits are calculated using the Helene method (Helene 1983). For nightly observations, these limits are typically on the order of (3–10) × 10^{-12} photons cm^{-2} s^{-1} above 300 GeV or 3%–8% of the steady Crab Nebula flux. When binned by orbital phase, the limits extend down to (2–6) ×10^{-12} photons cm^{-2} s^{-1} above 300 GeV or 2%–5% of the Crab Nebula. Particularly striking is the distinct lack of strong TeV emission during the apastron phases of ϕ = 0.5–0.8 as these are the orbital phases during which both MAGIC and VERITAS have previously detected strong (10%–20% Crab Nebula) emission.

Unexpectedly, in late 2010, gamma-ray emission from the source was detected over a region of the binary orbit previously undetected by TeV instruments (Ong et al. 2010). From 2010 September 17 to November 7 (MJD 55455–55507), a total of 13.9 hr on LS I +61° 303 were accumulated resulting in the detection of 129 excess events above background. This constitutes a detection at the 5.6σ post-trials significance level (5.7σ pre-trials significance with two trials for two sets of analysis cuts: standard analysis cuts and an analysis tailored

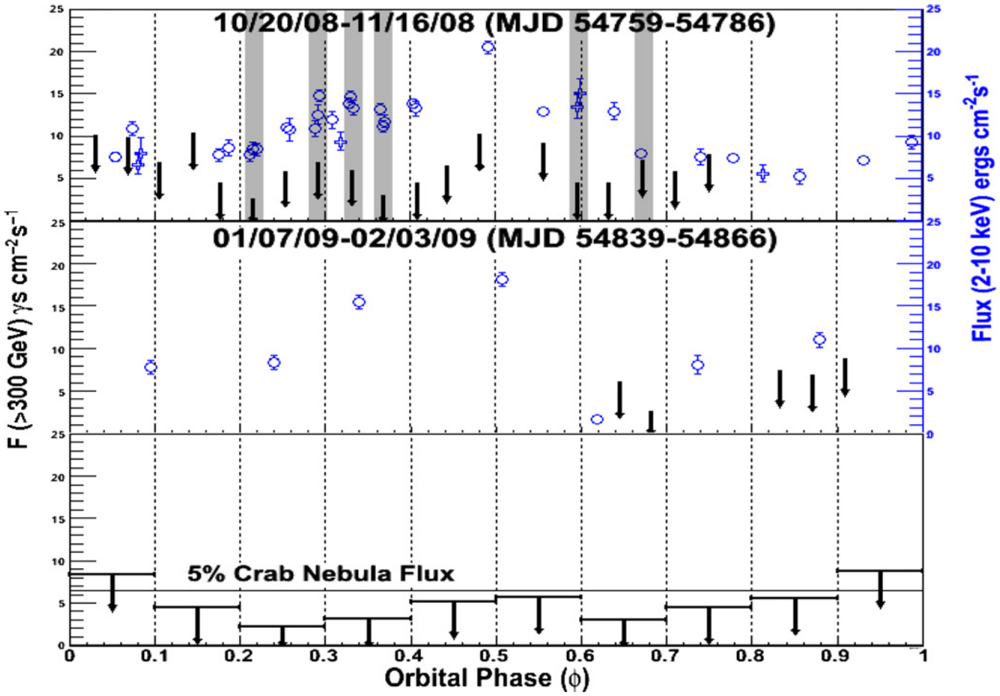

Figure 1. TeV flux upper limits from VERITAS (black points and arrows) compared to contemporaneous X-ray fluxes as measured by *Swift*–XRT (crosses) and *RXTE*–PCA (open circles). The bottom panel shows the integrated result from the two measured orbital cycles observed from 2008 October to 2009 February. VERITAS flux measurements with less than 3σ pre-trials significance are shown as 99% confidence flux upper limits. The shaded regions indicate observations which had directly overlapping X-ray measurements by either *RXTE* or *Swift*.

(A color version of this figure is available in the online journal.)

for harder spectrum sources). During phases 0.0–0.1 (close to superior conjunction at phase 0.081) the source was observed for a total of 4.2 hr. During this time a total of 66 excess events were recorded, corresponding to a 4.8σ post-trials (5.4σ pre-trials) significance (accounting for twenty trials accumulated by analyzing the data in 10 orbital phase bins with two sets of analysis cuts). Since this detection consists of too few events to construct a differential energy spectrum with comparable statistics to those previously published, we assume a spectral index of $\Gamma = 2.6$ (Acciari et al. 2008) in order to produce absolute fluxes. The source flux was measured as $(6.86 \pm 1.45) \times 10^{-12}$ photons cm^{-2} s^{-1} above 300 GeV, or approximately 5% of the Crab Nebula flux in the same energy range. The source presented the highest observed flux on 2010 October 8 (MJD 55477, $\phi = 0.07$) with 57 excess events detected in 2.8 hr of observations, corresponding to a 5.2σ post-trials (5.7σ pre-trials) significance, accounting for 20 trials accumulated by analyzing 10 individual nights with two sets of analysis cuts to search for the maximal flux. During these observations the source flux was measured as $(9.23 \pm 1.9) \times 10^{-12}$ photons cm^{-2} s^{-1} above 300 GeV or approximately 7% of the Crab Nebula flux.

It should be noted that after appropriate statistical trials are taken into account (for binning on nightly and orbital timescales) the detection during phase 0.0–0.1 and on 10/08/10 stand as the only statistically significant detections published by any TeV instrument since 2007. The fact that these detections were made over a region of the orbit not previously suspected to be an active TeV phase is of particular interest.

3. X-RAY OBSERVATIONS

The *RXTE*–PCA (Swank 1994) and *Swift*–XRT (see Gehrels et al. 2004; Burrows et al. 2005) data presented here were both obtained from the public data archive at http://heasarc.gsfc.nasa.gov/ and analyzed using the HEASOFT (v6.9) package (Blackburn 1995). For *RXTE*–PCA analysis, standard data quality selection and screening (using the "rex" script in FTOOLS) was performed. All available data were extracted using only the top layer of Proportional Counting Unit 2 in each observation. The XSPEC 12.6 software package (Arnaud 1996) was used to fit spectra with a simple absorbed power law, assuming a fixed absorbing hydrogen column density ($N_{\rm H}$) of 0.75×10^{22} cm^{-2} (Kalberla et al. 2005) between 3 and 10 keV and to extract fluxes in the 2–10 keV range. Fluxes were then deabsorbed using the Wisconsin photoelectric cross sections (Morrison & McCammon 1983), or the "wabs" model within XSPEC. Also, given that the PCA instrument on *RXTE* is known to give larger fluxes (on the order of 20%) on the same source than other more precise instruments (Tomsick et al. 1999), all the PCA fluxes quoted here have been reduced by a factor of 1.18 in order to provide a more accurate comparison to the *Swift*–XRT analysis.

For the *Swift*–XRT analysis, all data shown here were accumulated in "photon counting mode" and analyzed using the most recent *Swift*–XRT analysis tools with the HEASOFT 6.2 package. The data were screened with standard filtering criteria and reduced using the *xrtpipeline* task. Background and source spectra were accumulated from each individual observation using circular regions of radius 60″ and 20″, respectively. XSPEC 12.6 was used to fit accrued spectra in the 0.3–10 keV range using a simple, absorbed power law with the galactic hydrogen column density fixed at 0.75×10^{22} cm^{-2}. Flux values and associated 1σ statistical errors were then calculated by integrating the fitted spectra over the 2–10 keV range.

Flux values as seen by both instruments (Figures 1–3) show a high degree of variability with values of (2–25) $\times$ 10^{-12} erg cm^{-2} s^{-1}, consistent with other observations of

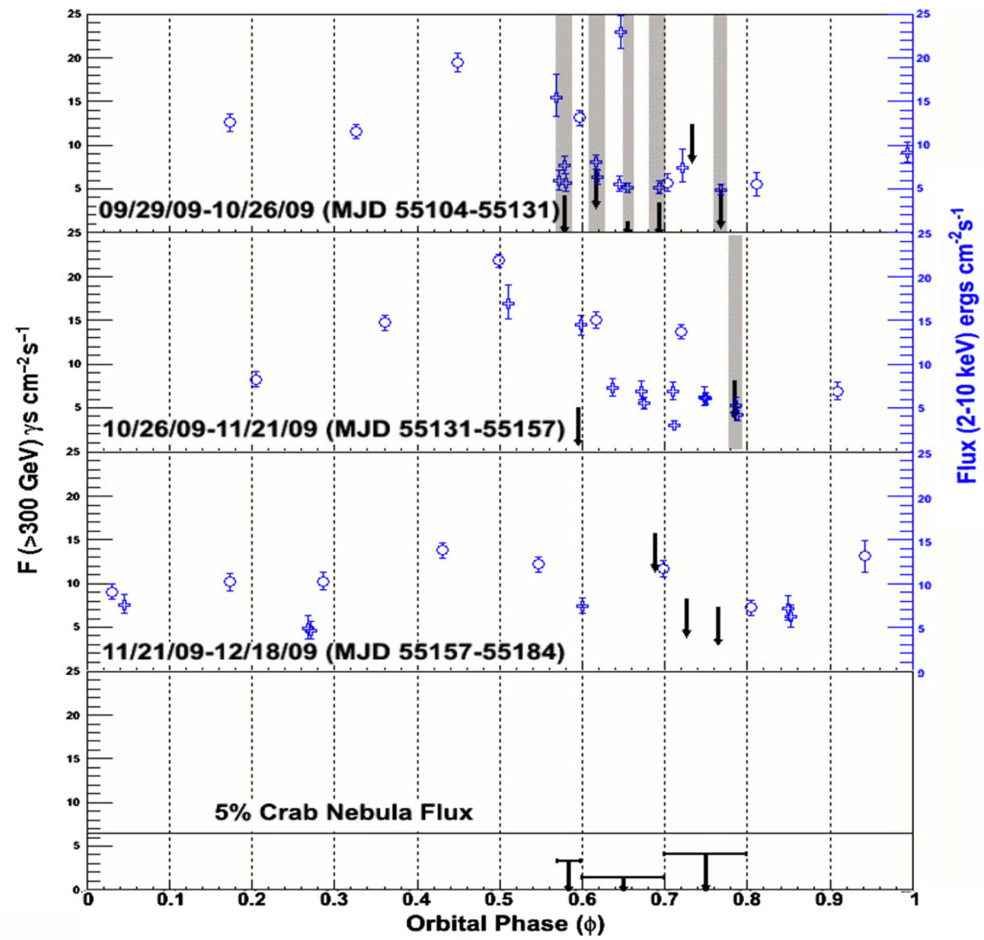

Figure 2. Same as Figure 1, but for the 2009–2010 observing season.
(A color version of this figure is available in the online journal.)

LS I +61° 303 with *RXTE*–PCA and *Swift*–XRT (i.e., Acciari et al. 2009).

Since variability of the X-ray emission from LS I +61° 303 has been demonstrated on various timescales, we select only data in the two bands which were directly overlapping in time, so as to provide an accurate test for any correlation with VHE emission. Additionally, all of the simultaneous X-ray observations were first checked to confirm that there was no evidence for X-ray variability within the observation. There are twenty simultaneous observations taken in both X-ray and TeV (gray shaded regions) in the data sets examined here; eight from *RXTE*–PCA observations and twelve from the *Swift*–XRT observations. As can be seen in Figure 4, while the X-ray flux varies significantly, none of the points correspond to a significant TeV detection. A test for correlation between the two data sets results in a Pearson product-moment correlation coefficient of -0.03 ± 0.23, which is consistent with two uncorrelated data sets.

We note that the TeV exposures are typically significantly longer than the corresponding X-ray observations. This is unavoidable, given the requirement that the TeV exposure be sufficient to achieve a useful sensitivity; however, it introduces the possibility that the (unmeasured) X-ray flux may have varied considerably within the TeV observation.

To test whether the correlation between X-ray and TeV emission presented in Anderhub et al. (2009) would have been measurable in the data presented here, we compared the Anderhub correlation fit between X-ray and TeV data points to our data. This fit, along with the Anderhub data points from which it was derived, is shown in Figure 4. Since the energy range of our X-ray observations was different than that presented in Anderhub et al. (2–10 keV versus 0.3–10 keV), we have converted the Anderhub fit to our energy range. This modification was derived by scaling the 0.3–10 keV flux range along a spectral fit with index of $\Gamma = 1.6$ (consistent with spectral measurements of the source found in Anderhub et al. 2009). Using this method, we arrive at a line fit of F(2–10 keV) $[10^{-12}$ erg cm^{-2} s$^{-1}] = (7.8 \pm 0.6) + (0.45 \pm 0.1) \times N(E > 300$ GeV) $[10^{-12}$ cm^{-2} s$^{-1}]$. According to this relation, the highest observed X-ray flux of $(14.7 \pm 0.7) \times 10^{-12}$ erg cm^{-2} s^{-1} leads to an expected TeV flux above 300 GeV of $15.3^{+7.1}_{-5.2} \times 10^{-12}$ photons cm^{-2} s^{-1} or approximately 10% of the Crab Nebula flux. For the overlapping observation in question, VERITAS observed the source for a total of 56 minutes and measured a negative fluctuation of events relative to background corresponding to a 99% Helene flux upper limit of 3.3×10^{-12} photons cm^{-2} s^{-1}, a factor of 4.6 lower than the predicted value.

We note that this flux prediction does not take into account the uncertainty in what VERITAS would have actually measured in the observation time quoted. However, even under conservative estimates of VERITAS sensitivity (5σ detection of a 5% Crab-type source in ~1 hr), a source on the level predicted by the Anderhub correlation used here would likely have yielded

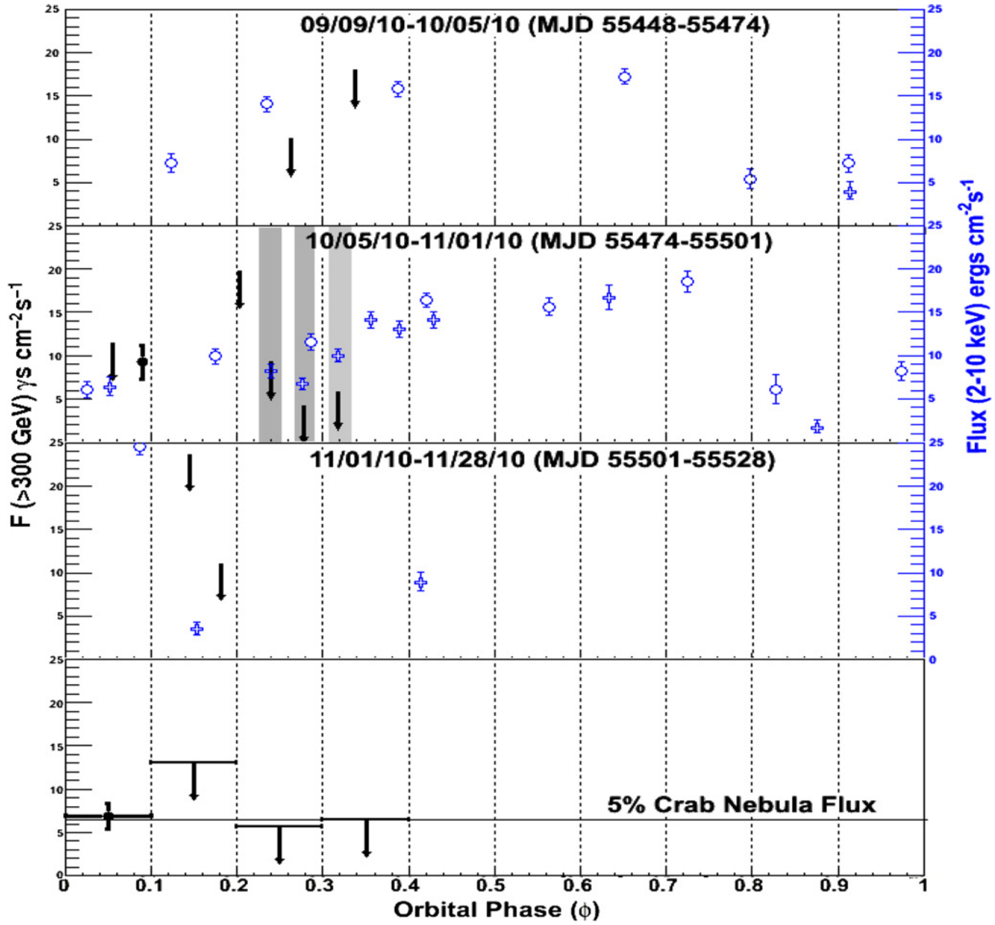

Figure 3. Same as Figure 1, but for the 2010–2011 observing season.
(A color version of this figure is available in the online journal.)

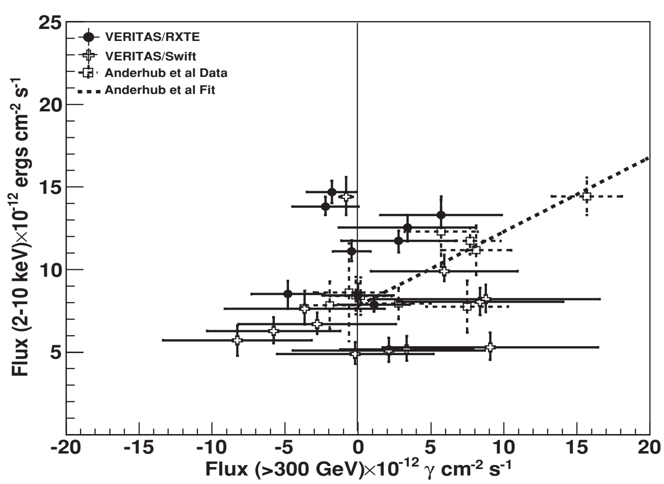

Figure 4. Comparison of the strictly simultaneously observed TeV and X-ray fluxes seen by VERITAS and *Swift*/*RXTE*, along with the data points and associated correlation fit from Anderhub et al. (2009).

strong evidence for a signal detection in the given observation livetime.

4. CONTEMPORANEOUS *FERMI*-LAT GeV OBSERVATIONS

We performed aperture photometry on the *Fermi*-LAT data set covering LS I +61° 303 for the periods during which VERITAS accrued observations from 2008 to 2010. Using the publicly available Fermi analysis tools and an aperture radius of 2°.4 (found to be optimal for this source in Abdo et al. 2009), we extracted the 100 MeV–300 GeV counts from the source in 26.5 day bins, and we used the *gtexposure* tools to calculate the exposure for each bin. Figure 5 shows the result of this analysis (without any background subtraction performed) along with the time periods during which VERITAS observed the source highlighted in gray regions. During each of the VERITAS observation windows indicated in the figure, VERITAS observed the source for typically 1–2 hr per night. The periods during which VERITAS successfully detected LS I +61° 303 in late 2010 (last three shaded regions in Figure 5) do not correspond to significantly higher or lower GeV flux than the previously observed regions during which VERITAS did not detect the source.

5. SUMMARY AND DISCUSSION

We have presented the results of TeV observations of the Galactic binary LS I +61° 303 made with the VERITAS array from 2008 October until 2010 December. These observations covered eight separate 26.5 day orbital cycles with coverage (though not uniform) of all orbital cycles. A comparison with previous observations of this source is useful. In Figure 6 all three years of observations presented in this paper, along with the previously obtained detections by both VERITAS and MAGIC (Acciari et al. 2008, 2009; Albert et al. 2008), are shown. In this figure, we plot only points from previous observations that had detections above 3σ along with the currently obtained flux upper

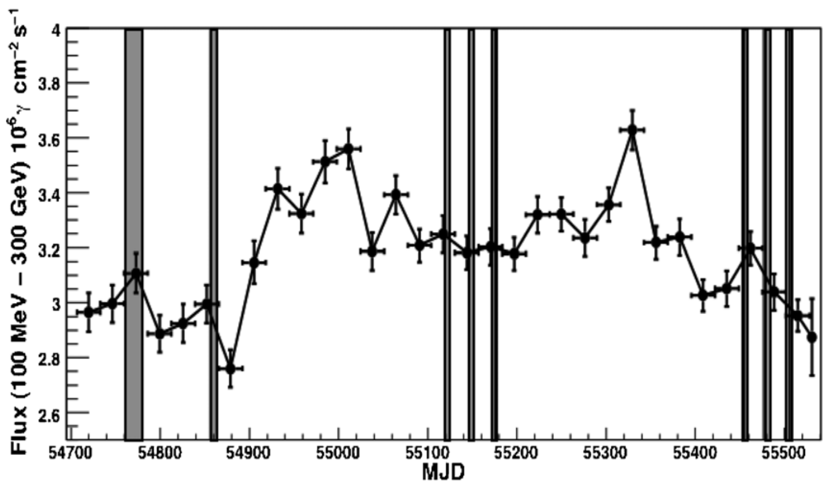

Figure 5. GeV flux observed by *Fermi*-LAT from LS I +61° 303 (with no background subtraction performed). The gray shaded regions show the times during which VERITAS observed the source during 2008–2010.

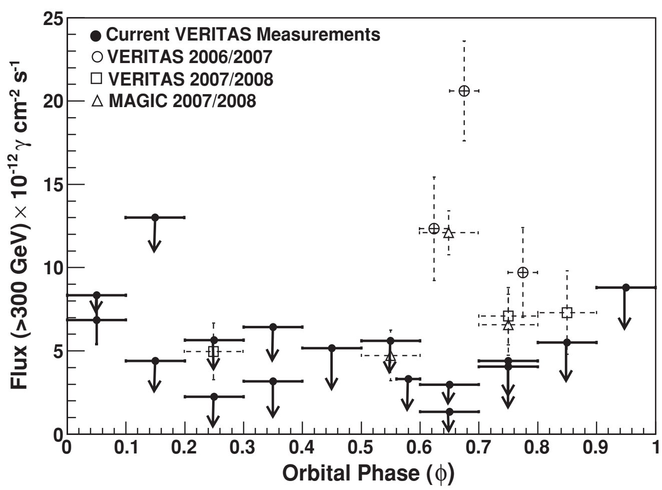

Figure 6. Observations presented in this paper (solid lines) along with previous observations (dashed lines) from Acciari et al. (2008, 2009) and Albert et al. (2008). Only detections at a significance larger than 3σ are shown from previous observations.

limits and detection near periastron. The previously published fluxes quoted at a different energy threshold were converted to >300 GeV fluxes using a spectral index of −2.5, consistent with published spectra of the source (Acciari et al. 2009). The data shown here do not indicate any significant evidence for TeV emission during the orbital phases previously detected by VERITAS and MAGIC (i.e., near apastron passage), with flux upper limits derived which are ∼2–3 times lower than the previously detected emission. Instead, the source has been detected for the first time during orbital phases 0.0–0.1, close to superior conjunction (at $\phi = 0.081$). A further implication of these observations is that there is no direct evidence that the process responsible for the detected *Fermi*-LAT emission continues beyond the published 6 GeV cutoff: all published spectra show only non-contemporaneous data.

An important caveat to these points is that we cannot rule out the existence of near-apastron TeV emission during the 2008–2010 timeframe. As is the case with all TeV observations, the sampling of the VHE flux from LS I +61° 303 was unavoidably limited, with observations taking place separated by days and only for integrations lasting several hours. Furthermore, since the orbital period of LS I +61° 303 (∼27 days) is very close to the lunar cycle, full-orbit observations of LS I +61° 303 with ground-based TeV telescopes are limited by their inability to observe during bright moon phases. The observations sampled only 8 orbits out of 27 covered by these two years, and observations in 2009–2010 focused exclusively on orbital phases $\phi = 0.5$–0.8. This leaves open the possibility that the source was active at VHE in some of the unobserved orbits during apastron passage. Also, the possibility exists that the sampling provided by the VERITAS observations simply missed the significant TeV activity.

We have also presented both contemporaneous and directly overlapping X-ray observations taken with *Swift*–XRT and *RXTE*–PCA. The 20 directly overlapping X-ray observations do not show any evidence for correlation with the TeV emission. This stands in contrast somewhat to the result of Anderhub et al. (2009), in which a correlation was detected between X-ray and TeV emission. However, the result of Anderhub et al. (2009) was obtained during a TeV outburst covering 60% of a single orbit, and this paper makes no claim of longer-term correlation between the two emission bands. We see no evidence for such a correlation during the observations taken here, which were obtained over several different orbital cycles.

During the 2008–2010 period, the GeV flux was monitored by *Fermi*-LAT. Dubois et al. (2011) have shown that the most recent *Fermi*-LAT GeV observations showed a marked flux increase, of ∼40%, in 2009 March, after which the previously clear orbital GeV flux modulation is no longer measurable. The result of Torres et al. (2010) shows that while the X-ray periodicity of the source is well defined, it is not entirely stable; the degree of modulation, and the phase of the peak of the emission, varies from orbit-to-orbit and year-to-year. These results, compounded by the TeV measurements in this paper, indicate that the non-thermal emission from LS I +61° 303 is not as stable as its southern hemisphere counterpart, LS 5039.

Torres et al. (2011) have suggested that the GeV emission characteristics can be simply explained by invoking a two-component model, where the observed flux is the result of magnetospheric (pulsar) emission, plus a wind contribution produced either in the inter-wind region and/or the pulsar wind zone. The magnetospheric contribution would be steady and exhibit a sharp spectral cutoff at ∼6 GeV, while the wind contribution would be expected to vary naturally with orbital phase. If the rate of particle acceleration is the main factor determining the GeV and TeV fluxes, then the observations reported here do not seem to support this idea in its simplest form. Since the wind component is expected to be sensitive to orbital modulation, and it provides the primary contribution to the TeV emission, the GeV flux increase since 2009 March should naturally lead to a larger fraction of the flux being modulated with the orbital period, and to increased TeV flux. The opposite of both of these effects is observed. Other factors may affect this conclusion, however; for example, increased inverse Compton cooling may cause the spectrum to steepen, enhancing the GeV flux and decreasing the TeV flux. The system may also have moved into a state where the Compton process has saturated, and the output spectrum is largely independent of the input photon flux, thus explaining the disappearance of orbital modulation.

How can this apparent long term variability be explained? The results of radio monitoring (Gregory 2002) show a definite modulation of the phase and peak flux density of the radio outbursts with a period of 1667 ± 8 days. In Gregory & Neish (2002) this effect is attributed to a model where a pulsar is embedded in a coplanar fashion within the equatorial disk of the Be star. The long term modulation then results from periodic enhancements of the stellar wind density within the disk. If this is the case, and the HE–VHE emission results from the same particle population as the radio emission, then perhaps the long term variation in these bands is not unexpected. It certainly seems likely, given the contrast with the stability of the orbital light curves of LS 5039 (Kishishita et al. 2009; Aharonian et al. 2006; Abdo et al. 2009), that variations in the circumstellar environment of the Be star play an important role in determining the variability of the observed emission. Sensitive TeV observations of LS I $+61^{\circ}$ 303 began only in 2005 September, while *Fermi* was launched in 2008 June. Continued monitoring over the coming years from X-ray to TeV will allow us to probe longer-term cycles, to study the cross-correlations in more detail and to characterize the emission spectra more precisely.

This research is supported by grants from the U.S. Department of Energy, the U.S. National Science Foundation, the Smithsonian Institution, by NSERC in Canada, by Science Foundation Ireland (SFI 10/RFP/AST2748), and by STFC in the U.K. We acknowledge the excellent work of the technical support staff at the Fred Lawrence Whipple Observatory and the collaborating institutions in the construction and operation of the instrument.

The submitted manuscript has been created by employees of UChicago Argonne, LLC, Operator of Argonne National Laboratory ("Argonne") in conjunction with the VERITAS collaboration. Argonne, a U.S. Department of Energy Office of Science laboratory, is operated under Contract No. DE-AC02-06CH11357. The U.S. Government retains for itself, and others acting on its behalf, a paid-up nonexclusive, irrevocable worldwide license in said article to reproduce, prepare derivative works, distribute copies to the public, and perform publicly and display publicly, by or on behalf of the Government.

J. Holder acknowledges the support of the NASA Fermi Cycle 2 Guest Investigator Program (grant number NNX09AR91G).

REFERENCES

Abdo, A. A., et al. 2009, ApJ, 701, L123
Abdo, A. A., et al. 2010, ApJS, 188, 405A
Acciari, V., et al. 2008, ApJ, 679, 1427
Acciari, V., et al. 2009, ApJ, 700, 2
Aharonian, F. A., et al. 2006, A&A, 460, 743
Albert, J., et al. 2006, Science, 312, 1771
Albert, J., et al. 2008, ApJ, 684, 1351
Anderhub, H., et al. 2009, ApJ, 706, L27
Aragona, C., et al. 2009, ApJ, 698, 514
Araudo, A. T., Bosch-Ramon, V., & Romero, G. E. 2009, A&A, 503, 673
Arnaud, K. A. 1996, in ASP Conf. Ser. 101, Astronomical Data Analysis Software and Systems V, ed. G. Jacoby & J. Barnes (San Francisco, CA: ASP), 17
Blackburn, J. K. 1995, in ASP Conf. Ser. 77, Astronomical Data Analysis Software and Systems IV, ed. R. A. Shaw, H. E. Payne, & J. J. E. Hayes (San Francisco, CA: ASP), 367
Burrows, D. N., et al. 2005, Space Sci. Rev., 120, 165
Casares, J., et al. 2005, MNRAS, 360, 1105
Dhawan, V., Mioduszewski, A., & Rupen, M. 2006, in Proc. Microquasars and Beyond: From Binaries to Galaxies, Proceedings of Science, Como, IT, ed. T. Belloni, 52
Dubois, R., et al. 2011, in Proc. 1st Sant Cugat Forum on Astrophysics, ICREA Workshop on the High-energy Emission from Pulsars and their Systems, Sant Cugat, Spain, 2010 April, ed. N. Rea & D. F. Torres (Berlin: Springer)
Dubus, G., Cerutti, B., & Henri, G. 2010, A&A, 516, A18
Fomin, V. P., et al. 1994, Astropart. Phys., 2, 137
Gehrels, N., et al. 2004, ApJ, 611, 1005
Gregory, P. C. 2002, ApJ, 525, 427
Gregory, P. C., & Neish, C. 2002, ApJ, 580, 1133
Greiner, J., & Rau, A. 2001, A&A, 375, 145
Harrison, F. A., Ray, P. S., Leahy, D. A., Waltman, E. B., & Pooley, G. G. 2000, ApJ, 528, 454
Helene, O. 1983, Nucl. Instrum. Methods Phys. Res., 212, 319
Hermsen, W., et al. 1977, Nature, 269, 494
Hutchings, J. D., & Crampton, D. 1981, PASP, 93, 486
Kalberla, P. M. W., Burton, W. B., Hartmann, D., Arnal, E. M., Bajaja, E., Morras, R., & Pöppel, W. G. L. 2005, A&A, 440, 775
Kishishita, T., Tanaka, T., Uchiyama, Y., & Takahashi, T. 2009, ApJ, 697, L1
Massi, M., Ribó, M., Paredes, J. M., Peracaula, M., & Estalella, R. 2001, A&A, 376, 217
Massi, M., & Zimmerman, L. 2010, A&A, 515, 82
Morrison, R., & McCammon, D. 1983, ApJ, 270, 119
Ong, R. A., et al. 2009, in Proc 31st ICRC, Lodz, Poland (arXiv:0912.5355)
Ong, R. A., et al. 2010, ATel, 2948
Perkins, J. A., et al. 2009, Fermi Symposium, eConf Proceedings, C091122
Romero, G. E., Okazaki, A. T., Orellana, M., & Owocki, S. P. 2007, A&A, 474, 1522
Sierpowska-Bartosik, A., & Torres, D. 2009, ApJ, 693, 1462
Smith, A., Falcone, A., Holder, J., Kaaret, P., Maier, G., & Pandel, D. 2009, ApJ, 693, 1621
Swank, J. H. 1994, in Proc. 181st American Astronomical Society Meeting, Vol. 185, Phoenix, AZ, 6701
Tavani, M., Kniffen, D., Mattox, J. R., Paredes, J. M., & Foster, R. 1998, ApJ, 497, L89
Tomsick, J. A., Kaaret, P., Kroeger, R. A., & Remillard, R. A. 1999, ApJ, 512, 892
Torres, D., et al. 2010, ApJ, 719, L104
Torres, D., et al. 2011, ed. N. Rea & D. F. Torres in Proc. 1st Sant Cugat Forum on Astrophysics, ICREA Workshop on the High-energy Emission from Pulsars and their Systems, Sant Cugat, Spain, 2010 April (Berlin: Springer) (arXiv:1008.0483)